JOURNAL OF MATERIALS SCIENCE 19 (1983) 1576–1595

Relaxation in elastic and viscoelastic materials

ROBERT M. HILL, LEONARD A. DISSADO
The Dielectrics Group, Chelsea College, University of London, Pulton Place, London SW6 5PR, UK

The mechanical compliance and modulus retardation/relaxation functions are examined in terms of a general behaviour which contains more than one process. An analytical approach to the transformation in the anelastic response between the compliance and the modulus is derived and applied to a cooperative model of relaxation behaviour. In particular it is shown that mechanical viscoelasticity is equivalent to the anomalous low frequency dispersion process that has been observed in dielectrics containing quasi-free charges. Comparison with published experimental data over a wide range of solid materials shows the validity of the cooperative model to mechanical relaxation.

1. Introduction

The conventional approach to the viscoelastic response in materials is to consider a distribution of Debye-like relaxing elements each with its own relaxation time [1, 2]. Investigation of the experimental data then gives the distribution of these elements either as a retardation spectrum, from compliance measurements, or a relaxation spectrum, from modulus measurements. In principle neither of these spectra contains more information than the original data as they are simply mathematical transforms of the original, invariably non-Debye, measurements. Furthermore it has been found that the relaxation and retardation spectra for the same material are different [1] and that neither appears to relate directly to other physical properties of the system such as the distribution of molecular weights in polymers [2].

A number of empirical relaxation functions have been proposed [2–6] and have been applied to specific samples of materials. The feature of these response functions that has not been generally appreciated is the appearance of fractional power law relationships between the mechanical response and the frequency [7]. Recently a cooperative theory of relaxation in dielectrically active materials has been proposed [8–10] by the present authors and in this theory such fractional power law behaviour is a direct result of two independent types of cooperative behaviour in the material under study. It is our intention here to examine the general relaxation response functions, to apply the results of the cooperative theory to these functions, and to compare the predicted behaviour with that given by experimental data measured in a range of materials using a number of different mechanical relaxation techniques.

In order to carry out the comparison with experimental data it was found necessary to re-develop the macroscopic approach to retardation and relaxation, in particular to consider that more than one relaxation process can occur in the material. This development is contained in Section 2. In Section 3 this approach is applied to the cooperative model by making use of the direct analogy between dielectric relaxation and compliance retardation [1, 11]. Exact cooperative response functions are obtained for stress retardation and the analytic transformation of Section 2 is used to determine the strain relaxation response. In the following section the applicability of the cooperative model as a description of real, experimental, relaxation is investigated and it is shown that excellent agreement can be obtained in the anelastic region. One particular feature of the approach followed here is the recognition of

0022–2461/84 $03.00 + .12

the exact equivalence between the viscoelastic behaviour of polymeric materials at temperatures in excess of the glass transition temperature and the anomalous low frequency behaviour that has been observed dielectrically in materials that contain quasi-free charges [12], usually ions, such as the fast-ion conductors. These processes are quite distinct from perfect viscosity, which is itself equivalent to a d.c. electrical conductivity, although they are commonly poorly distinguished.

2. Retardation and relaxation

2.1. Constitutive equations

We consider a homogeneous and isotropic material and apply a step increase in shear stress of magnitude $\Delta\sigma$ at time zero. The response from a single relaxation process to this step at a later time t can be expressed in terms of the resultant strain as

$$\Delta\alpha(t) = \Delta\sigma \cdot \phi(t) \tag{1}$$

where the creep retardation function for the process, $\psi(t)$, is defined by

$$\psi(t) = \phi(t) - \phi(0) \tag{2}$$

to be zero at time zero. When the stress is not a simple step function of time but continuously varying the contribution to the stress from the time interval Δt is

$$\Delta\sigma = \frac{\mathrm{d}\sigma(t)}{\mathrm{d}t}\Delta t \tag{3}$$

from which, by summing over all contributions in time and allowing for a finite stress, $\sigma(-\infty)$, at $t = -\infty$,

$$\alpha(t) = \sum_k \frac{\mathrm{d}}{\mathrm{d}t_k}\{\sigma(t_k)\}\,\Delta t_k \phi(t - t_k) + \sigma(-\infty)\phi(\infty) \tag{4a}$$

For the particular process under consideration the summation can be replaced, in the limit of small Δt_k, by an integral to give

$$\alpha(t) = \int_{-\infty}^{t} \dot{\sigma}(t_1) \cdot \phi(t - t_1)\,\mathrm{d}t_1 + \sigma(-\infty)\phi(\infty) \tag{4b}$$

where the dot notation is used throughout to indicate differentiation of a function $f(x)$ with respect to the variable x.

In real systems there is usually more than one process of relaxation and these can be distinguished by the time scale on which they occur. For processes slower than the particular one that is under consideration no relaxation takes place during the observation process, but systems responding on a shorter time scale will be completely relaxed throughout the observation period. We can represent the summation of the relaxed processes by adding their contribution to the strain in the form $\sigma(t) \cdot \phi_i(\infty) = \alpha_i$, the instantaneous strain, to obtain

$$\alpha(t) = \alpha_i + \sigma(-\infty)\phi(\infty) + \int_{-\infty}^{t} \dot{\sigma}(t_1)\phi(t - t_1)\,\mathrm{d}t_1 \tag{5}$$

Integration by parts then gives

$$\alpha(t) = \alpha_i + \sigma(t)\phi(0) + \int_{-\infty}^{t} \sigma(t_1)\dot{\phi}(t - t_1)\,\mathrm{d}t_1 \tag{6}$$

in which $\phi(0)$ is commonly referred to as the instantaneous response of the process under consideration. By change of variables in Equations 5 and 6 these equations can be expressed in the equivalent forms

$$\alpha(t) = \alpha_i + \sigma(-\infty)\phi(\infty) + \int_0^{\infty} \dot{\sigma}(t - u)\phi(u)\,\mathrm{d}u \tag{7}$$

and

$$\alpha(t) = \alpha_i + \sigma(t)\phi(0) + \int_0^{\infty} \sigma(t - u)\dot{\phi}(u)\,\mathrm{d}u \tag{8}$$

Equations 5 to 8 are the Duhamel integrals [13] with $\phi(t)$ termed the creep compliance or retardation function for the process. Equation 6, under conditions of constant strain, defines a flow property and hence $\mathrm{d}\phi(t)/\mathrm{d}t$ can be termed a retardation current in analogy with dielectric relaxation [2, 11]. Fig. 1a shows, schematically, the time dependent strain response to a step function applied stress and includes a viscosity term, η, for generality.

In a similar manner we can consider the material responding to a time-dependent strain. In this case it is necessary to examine the initial conditions with some care. For a step function increase in strain the initial response will be a step function increase in stress, of large magnitude. As before we single out the particular process to be examined as occurring in the time scale that is of interest. The other relaxation processes which occur on a shorter time scale reduce the "instantaneous" value of stress to the unrelaxed value [14] for the process which is under consideration, which then relaxes the stress further, but not

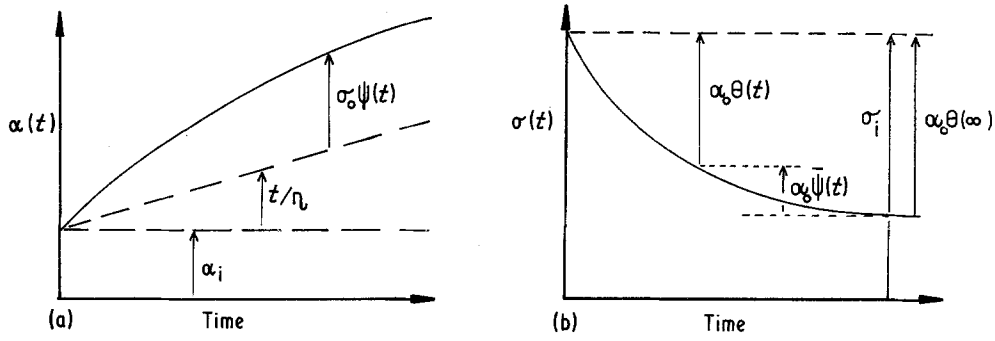

Figure 1 Diagrammatic representation of the time dependence of (a) strain retardation and (b) stress relaxation for step function excitation. σ is the stress, α is the strain and η is the time-independent viscosity.

necessarily completely. The characteristic values of stress are therefore the effective initial stress, σ_i, and the infinite time relaxed value, $\sigma(\infty)$, which is attained after the process of interest has relaxed the system. At a time t the observed stress for a general strain is obtained by a similar approach to that contained in Equations 1 to 4 as

$$\sigma(t) = \sigma_i - \alpha(-\infty)\theta(\infty) - \int_{-\infty}^{t} \dot{\alpha}(t_1)\theta(t-t_1)\,dt_1 \tag{9}$$

where the term $\alpha(-\infty)\theta(\infty)$ again represents the contribution of the process under consideration from a strain existing at the onset of the experiment. A second set of Duhamel integrals can be developed from Equation 9 but the one which is of direct use here is

$$\sigma(t) = \sigma_i - \alpha(t)\theta(0) - \int_{-\infty}^{t} \alpha(t_1)\dot{\theta}(t-t_1)\,dt_1 \tag{10}$$

Considering now a step increase in strain from zero to α_0 at zero time, Equation 10 can be expressed as

$$\sigma(t) = \sigma_i - \alpha_0\theta(0) - \int_{0}^{t} \alpha_0\dot{\theta}(u)\,du \tag{11}$$

which gives

$$\sigma(t) = \sigma_i - \alpha_0\theta(t) \tag{12}$$

If now we let

$$\bar{\psi}(t) = \theta(\infty) - \theta(t) \tag{13a}$$

then

$$\sigma(t) = \alpha_0\bar{\psi}(t) + \sigma_i - \alpha_0\theta(\infty) \tag{13b}$$

The function $\bar{\psi}(t)$ is commonly called the relaxation function but, as indicated above and in Fig. 1b, is not ideally suited to describe stress relaxation as it has been artificially set to zero at infinite time. The more useful functions are the relaxation modulus, $\theta(t)$, and the relaxation memory function, $d\theta(t)/dt$ $(= -d\bar{\psi}(t)/dt)$. Equations 5 to 8 and Equations 9 and 10 are constitutive equations and express the response of the system to two different types of experimental techniques. Fig. 1 indicates, in diagrammatic form, the physical significance of the terms within these equations for the cases of both constant applied stress and constant applied strain where both the stress and the strain are applied at zero time.

In a linear system, which we shall consider, the steady state stress and strain are proportional giving the compliance of the material as the ratio of the strain to the stress, and the modulus as the ratio of the stress to the strain. These definitions can be extended to the time domain by considering the time dependent compliance and modulus as given by

$$J(t) = \alpha(t)/\sigma(t) \quad \text{and} \quad M(t) = \sigma(t)/\alpha(t) \tag{14}$$

respectively. The latter is commonly used in the description of the elastic properties of materials whereas under conditions of steady state shear flow in a liquid the compliance approach can be used to define the steady state viscosity, η, through Newton's relationship

$$\eta^{-1} = \alpha/\dot{\sigma} \tag{15}$$

Since the advent of polymeric materials the distinction between these two classes has become less obvious. The general group of materials which exhibit partial elastic recovery and partial flow are termed viscoelastic. The particularization of the modulus and compliance functions in Equations 14 to non-isotropic materials has received considerable attention, a clear development is contained in [14], but will not be considered here. Instead

we shall consider the inter-relationships between the relaxation and retardation functions in the rest of the present section.

2.2. Time and frequency response

The linear response to a step function shear stress can be expressed as

$$J(t) = \alpha(t)/\sigma \quad \text{with} \quad \begin{array}{l} \sigma = 0 \quad \text{for } t < 0 \\ \sigma = \sigma_0 \quad \text{for } t \geqslant 0 \end{array} \tag{16}$$

and the linear response to a step function strain as

$$M(t) = \sigma(t)/\alpha \quad \text{with} \quad \begin{array}{l} \alpha = 0 \quad \text{for } t < 0 \\ \alpha = \alpha_0 \quad \text{for } t \geqslant 0 \end{array} \tag{17}$$

Noting that Equation 2 contains the condition that at zero time the creep compliance is zero and allowing for a Newtonian viscosity under creep conditions we have from Equation 6, when $(t - t_1)$ is set equal to u,

$$J(t) = (\alpha_i/\sigma_0) + J_0 \int_0^t \dot{\phi}(u)\,du + \int_0^t (\eta)^{-1}\,du + J_0\phi(0) \tag{18}$$

$$= J_i + J_0\phi(t) + (t/\eta) \tag{19}$$

where J_i is the "initial" response due to the short time scale processes and J_0 is the magnitude of the increment of the time-dependent compliance from the process under consideration. From Equation 12 we have that

$$M(t) = M_i - M_0\theta(t) \tag{20}$$

where M_i is the initial, faster process relaxed, response and M_0 is the magnitude of the time-dependent modulus decrement. With generality a viscous term could appear in Equation 20 but this has been suppressed for, in the presence of a non-infinite viscosity, the modulus relaxes through the viscosity as well as through the relaxation process, as will be shown in Section 3.2. In Equations 19 and 20 the amplitudes J_0 and M_0 have been abstracted as factors from the functions $\phi(t)$ and $\theta(t)$, which therefore become dimensionless.

The response of the system to an oscillatory stress/strain, the anelastic response, can be determined from the principle of superposition as

$$J(\omega) = \mathscr{F}\frac{\mathrm{d}}{\mathrm{d}t}J(t) \quad \text{and} \quad M(\omega) = \mathscr{F}\frac{\mathrm{d}}{\mathrm{d}t}M(t) \tag{21}$$

where $\mathscr{F}$ indicates a one-sided Fourier transformation. Applying the transform to Equation 19 gives

$$J(\omega) = \mathscr{F}\left(\frac{\mathrm{d}}{\mathrm{d}t}(J_i) + J_0\dot{\phi}(t) + \frac{1}{\eta}\right) \tag{22}$$

$$= J(\infty) + J_0F(\omega) - i(\omega\eta)^{-1} \tag{23}$$

in which, following experimental observation, we have replaced the Fourier transform of the delta function $(\mathrm{d}J_i/\mathrm{d}t)$ by the "infinite frequency" compliance $J(\infty)$. The function $F(\omega)$ is a complex spectral response function which becomes purely real and of magnitude unity at zero frequency and zero at infinite frequency.

Application of the Fourier transformation to Equation 20 yields

$$M(\omega) = \mathscr{F}\left(\frac{\mathrm{d}}{\mathrm{d}t}M_i - M_0\dot{\theta}(t)\right) \tag{24}$$

$$= M(\infty) - M_0G(\omega) \tag{25}$$

where $M(\infty)$ is the zero time, "infinite frequency", unrelaxed modulus [14] and $G(\omega)$ is a complex function with a real magnitude of unity at zero frequency and zero at infinite frequency. In the absence of a viscosity term, that is for infinite viscosity, examination of the relative phase of the driving and driven components of stress and strain show that [1, 2, 14]

$$J(\omega)\cdot M(\omega) = 1 \tag{26}$$

which gives a technique for transforming between the compliance and modulus functions. In the remainder of this section we examine this relationship.

2.3. Convolution integral

Substituting Equations 22 and 24 into Equation 26 gives

$$\mathscr{F}\left[\frac{\mathrm{d}}{\mathrm{d}t}J_i + J_0\dot{\phi}(t)\right] \times \mathscr{F}\left[\frac{\mathrm{d}}{\mathrm{d}t}M_i - M_0\dot{\theta}(t)\right] = 1 \tag{27}$$

which can be written in the forms

$$\mathscr{F}\frac{\mathrm{d}}{\mathrm{d}t}[J_i/J_0 + \phi(t) - \phi(0)] \times \mathscr{F}\frac{\mathrm{d}}{\mathrm{d}t}[M_i/M_0 - \theta(t)] = (J_0M_0)^{-1} \tag{28}$$

and

$$\int_0^t [J_i/J_0 + \phi(t) - \phi(0)] \times [M_i/M_0 - \theta(t-\tau)]\,\mathrm{d}\tau = -t/(J_0M_0) \tag{29}$$

in which Equation 29 is the convolution integral of the retardation and relaxation functions. If these functions are mathematically simple then either Equation 28 or Equation 29 can be a useful means of obtaining a compliance/modulus transformation. In general, however, for non-trivial cases, the solution of these equations can prove difficult.

2.4. Analytic solution

An alternative approach to the compliance/modulus transformation is to substitute Equations 23 and 25 into Equation 26 to obtain

$$[J_0F(\omega) + J(\infty)] \times [M(\infty) - M_0G(\omega)] = 1 \tag{30}$$

in which, once again, we consider only the infinite viscosity case. One particular case of Equation 26 is

$$J(\infty) \cdot M(\infty) = 1 \tag{31}$$

which, on substitution back into Equation 30, gives

$$-J_0M_0F(\omega)G(\omega) + J_0M(\infty)F(\omega) - J(\infty)M_0G(\omega) = 0 \tag{32}$$

from which the magnitude of the modulus dispersion decrement can be obtained in terms of the compliance dispersion parameters by taking the zero frequency limiting values of $G(\omega)$ and $F(\omega)$. It is simple to show that

$$M_0 = M(\infty)\frac{J_0}{J_0 + J(\infty)} \tag{33}$$

which gives the magnitude of the relaxed modulus as

$$M(0) = M(\infty) - M_0 = [J_0 + J(\infty)]^{-1} = J(0)^{-1} \tag{34}$$

which contains a second particular case of Equation 26 and indicates that as $J(0)$ is always positive the magnitude of the modulus cannot become negative, that is $M_0 < M(\infty)$.

Using these values the spectral response functions can be determined from Equation 32 as

$$[G(\omega)]^{-1} = \frac{J(\infty)}{J(0)}\left\{[F(\omega)]^{-1} + \frac{J_0}{J(\infty)}\right\} \tag{35}$$

and

$$[F(\omega)]^{-1} = \frac{M(\infty)}{M(0)}\left\{[G(\omega)]^{-1} - \frac{M_0}{M(\infty)}\right\} \tag{36}$$

giving the modulus response in terms of the compliance as

$$M(\omega) = M(\infty) - M_0G(\omega) = M(\infty)\left(1 - \frac{J_0}{J(\infty)}\left\{[F(\omega)]^{-1} + \frac{J_0}{J(\infty)}\right\}^{-1}\right) \tag{37a}$$

and the compliance response in terms of the modulus as

$$J(\omega) = J_0F(\omega) + J(\infty) = J(\infty)\left(1 + \frac{M_0}{M(\infty)}\left\{[G(\omega)]^{-1} - \frac{M_0}{M(\infty)}\right\}^{-1}\right) \tag{37b}$$

One feature contained in Equations 37 which is not obvious is that the maxima in the loss components of the compliance and modulus do not necessarily occur at the same frequency. Furthermore the ratio of the frequencies of maximum losses is dependent on the *relative* magnitude of the dispersion increment/decrement of the process being considered. Defining the relative magnitude of the dispersion as γ where

$$\gamma = \frac{J(\infty)}{J(0)} = \frac{M(0)}{M(\infty)} \quad \text{where } 1 \geqslant \gamma \geqslant 0 \tag{38}$$

and assuming the Debye spectral function as the simplest form of $F(\omega)$, that is

$$F(\omega) = \frac{1}{1 + i\omega/\omega_{p,J}}$$

where ω is the frequency and $\omega_{p,J}$ the frequency of peak loss for the compliance, the peak in the loss component of the modulus can be shown to occur at the frequency

$$\omega_{p,M} = \omega_{p,J} \cdot (\gamma)^{-1} \geqslant \omega_{p,J} \tag{39}$$

Equations 38 and 39 indicate that a large dispersion in either compliance or modulus is accompanied by a large frequency shift in the peak loss. Further, it can be shown that the assumption of a Debye function for $G(\omega)$ recovers Equation 39. Hence it is a general feature of the compliance/modulus transformation of a retardation/relaxation process in the absence of a viscous-like flow that the peak loss in the modulus spectrum lies at a *higher* frequency than that of the compliance spectrum.

In the particular case where the dispersion is small, that is as γ approaches unity, Equations 37 give

$$F(\omega) \simeq G(\omega) \tag{40}$$

Unfortunately this simple and convenient result cannot be taken as being of general applicability although it is certainly likely to apply under acoustic absorption conditions where the real part of the dispersive process is seen as a small change in the velocity of the acoustic wave.

3. Cooperative relaxation and retardation

3.1. Relaxation behaviour

It is generally accepted, as discussed in [1, 2], that there is a formal correspondence between the compliance functions of mechanical relaxation and the susceptibility functions of dielectric relaxation. Section 2b, by considering the infinite frequency compliance, extends the correspondence to the dielectric permitivity as $J(\infty)$ is equivalent to ϵ_∞, the "infinite frequency" permittivity. Table I lists the dielectric, compliance and modulus functions, in terms of the notation and approach used here. There is, however, one essential difference in the behaviour. In the dielectric case a response can be observed even when there is no dielectric material between the plates of the test capacitor. This is the vacuum response and due to the change in plate charge. The absolute vacuum value for the permittivity, ϵ_0, allows the permittivity of all materials to be expressed in relative, dimensionless, units. In the mechanical cases there is no equivalent to the vacuum response, a vacuum cannot withstand a mechanical stress, and hence it is not possible to define either compliance or modulus in relative terms. The vacuum response, furthermore, is a true instantaneous response and is one component of the infinite frequency permittivity. In practical mechanical systems inertia negates even the possibility of a similar true instantaneous response. However when materials are being investigated in a particular time or frequency range the combined response of *all* processes which occur on shorter time scales, and hence at higher frequencies, result in the measurable values of $J(\infty)$ and $M(\infty)$, as already discussed. The exact equivalence to these processes can be seen in the dielectric response where the measured value of ϵ_∞ for the kHz range, for example, is invariably greater than the square of the refractive index which is, in turn, greater than unity, indicating the presence of more than one dispersion process.

The authors have proposed a cooperative theory of dielectric relaxation [8–10] which has recently been re-cast into a cluster model form [15, 16]. It has also already been shown [17] that the spectral response function derived from the cooperative model is applicable to compliance data over a range of material types. In this section the mechanical equivalences to the cooperative dielectric functions will be obtained although the discussion of the model of mechanical response will be deferred to a later article.

Consideration of the cooperative model has resulted in a description of the dielectric relaxation current, Table I, in the form [8, 15, 16]

TABLE I Comparison of dielectric and mechanical relaxation functions

Dielectric	Compliance	Modulus
Applied electric field, $E(t)$	Applied stress, $\sigma(t)$	Applied strain, $\alpha(t)$
Resultant polarization, $P(t)$	Resultant strain, $\alpha(t)$	Resultant stress, $\sigma(t)$
Dielectric susceptibility,	Mechanical compliance,	Mechanical modulus,
$\chi = \mathrm{d}P/\mathrm{d}E$	$J = \mathrm{d}\alpha/\mathrm{d}\sigma$	$M = \mathrm{d}\sigma/\mathrm{d}\alpha$
Relaxation current, $j(t) = \mathrm{d}P/\mathrm{d}t$	Retardation current, $J_0\,\mathrm{d}\phi/\mathrm{d}t$	Memory function, $M_0\,\mathrm{d}\theta/\mathrm{d}t$
Permittivity,	Anelastic compliance,	Anelastic modulus,
$\epsilon(\omega) = \chi(\omega) + \epsilon_\infty$ $= \chi(0)\cdot F(\omega) + \epsilon_\infty$	$J(\omega) = J_0 F(\omega) + J(\infty)$	$M(\omega) = M(\infty) - M_0 G(\omega)$
Electrical resistance,	Viscosity,	Viscous loss,
$R = E_{\mathrm{dc}}/j_{\mathrm{dc}}$	$\eta = (\alpha)^{-1}\,\mathrm{d}\sigma/\mathrm{d}t$	$V_0 g(\omega)$
Time dependence of polarization,	Creep retardation function,	Stress relaxation function,
$P(t) = P(0)\cdot f(t)$	$\psi(t) = \phi(t) - \phi(0)$	$\bar{\psi}(t) = \theta(\infty) - \theta(t)$

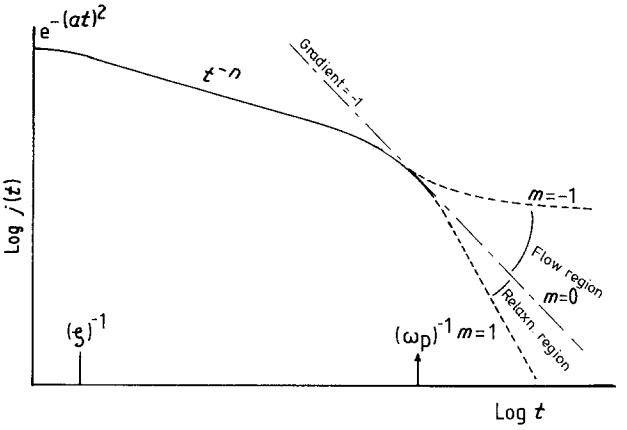

Figure 2 Schematic representation of the complete cooperative decay function of Equation 41. ζ is the characteristic frequency at which the Gaussian limiting behaviour gives way to the first power law decay region and ω_p is the characteristic rate for the relaxation process under observation. It can be seen that the long time limiting case with the observed value of m equal to -1 corresponds to a time-independent d.c. conductivity. Both the relaxation and flow regions of behaviour at long times are indicated.

$$j(t) \propto (\omega_p t)^{-n} \exp(-\omega_p t)\,{}_1F_1(1-m; 2-n; \omega_p t) \qquad \zeta t > 1 \qquad (41a)$$

and

$$j(t) \propto \exp(-at^2) \qquad \zeta t < 1 \qquad (41b)$$

where ω_p is the characteristic relaxation rate of the dielectric process under investigation, ${}_1F_1(\ ;\ ;\ )$ is the confluent hypergeometric function [18, 19] and m and n are fractional correlation indices for the intra- and inter-cluster cooperative relaxations that give the complete response [8]. The short time behaviour of Equation 41a is dominated by the intra-cluster relaxation with a time development of the asymptotic form $(\omega_p t)^{-n}$, for times greater than a value ζ^{-1} appropriate to the local structure, where ζ^{-1} is expected to lie in the range 10^{-12} to 10^{-11} sec. This behaviour lasts until times of the order of the reciprocal of the relaxation rate after which inter-cluster relaxations dominate giving an asymptotic decay of the form $(\omega_p t)^{-(1+m)}$. In the transition region, that is for $\omega_p t \simeq 1$, a limited region of exponential-like behaviour is found, and at very short times, $t < \zeta$, the zero time value of the current is approached as a Gaussian, Equation 41b, so that there is no divergence of the current at zero time. The magnitudes of the correlation indices m and n are always positive and less than unity. Relaxation, as indicated in Fig. 2, is characterized by current decay power law behaviour with experimentally observed values of m and n that are positive.

A recent development of the cooperative theory [20] has shown that the experimentally observed value of m can be negative. This is a result of correlated *flow* of charges in the material. In this case the long time asymptotic behaviour of the current takes the form $(\omega_p t)^{-(1-|m|)}$, giving the apparent anomaly in the sign of m. As shown in Fig. 2 this behaviour, as the magnitude of m approaches unity, can be mistaken for the onset of a d.c. conductivity but as long as the magnitude is not exactly unity it is correctly described by the anomalous low frequency dispersion process [12] which has been observed experimentally in fast ion conductors and other materials in which charge flow is essentially ionic and which leads to a large low frequency dispersion in *both* the real and imaginary parts of the permittivity. From Table I it can be seen that the function represented schematically in Fig. 2, the time-dependent relaxation current, is equivalent to the time evolution of the compliance retardation function $\dot{\phi}(t)$. Hence we expect two different forms of mechanical response, one corresponding to the relaxation region of behaviour with the observed value of m being positive and the second to the flow region with the observed value of m taking a negative value.

One-sided Fourier transformation of Equation 41 gives the dielectric susceptibility spectral function in the form

$$\chi(\omega) = \chi(0) \cdot \left(1 + i\frac{\omega}{\omega_p}\right)^{-(1-n)} \times {}_2F_1\left(1-n, 1-m; 2-n; \frac{1}{1+i\omega/\omega_p}\right) \qquad (42)$$

where $\chi(0)$ is the zero frequency magnitude of the susceptibility, and is real. It is Equation 42 that has been shown to be applicable to the observed spectral response of the compliance [17] and hence we shall use it as the basis for the determination of the mechanical response functions. Equation 42 can be re-expressed directly in

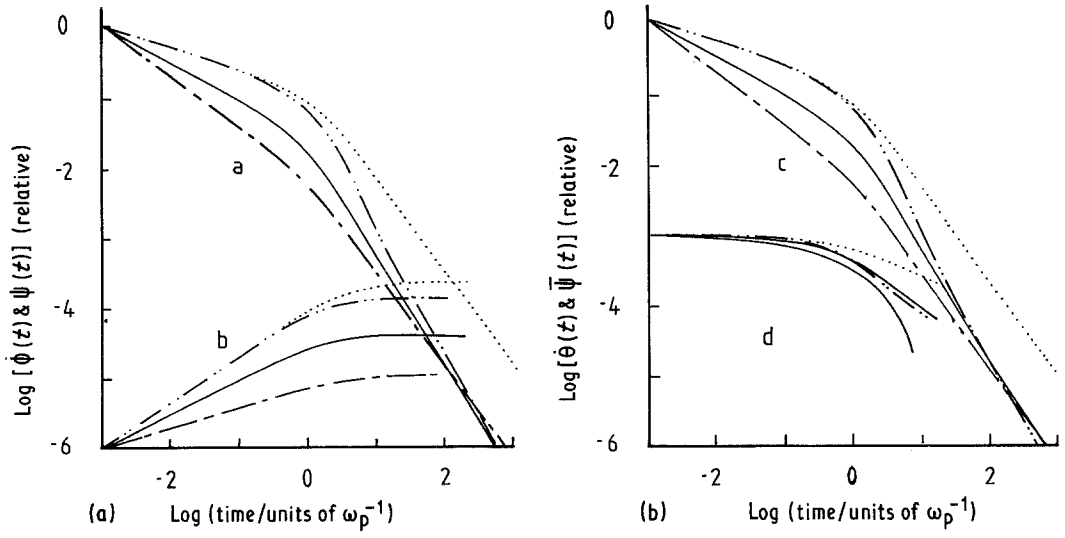

Figure 3 Computed plots of (a) the retardation current, (b) the creep retardation function, (c) the relaxation memory function, and (d) the relaxation function from Equations 40 and 45 using the following values of the correlation parameters: ——— $m = n = 0.5$; — — — — $m = 0.3, n = 0.7$; — — — — — — $m = 0.7, n = 0.3$; and ····· $m = n = 0.3$.

the compliance spectral response form as

$$F(\omega) = F_0(1+ix)^{-(1-n)} \times {}_2F_1\left(1-n, 1-m; 2-n; \frac{1}{1+ix}\right) \quad (43)$$

by letting $x = \omega/\omega_{p,J}$ be the reduced frequency and F_0 a normalizing parameter such that $F(\omega = 0)$ is unity, as required by Equation 23. F_0 is then given by

$$F_0 = \Gamma(1-n+m)/[\Gamma(m)\cdot\Gamma(2-n)] \quad (44)$$

where $\Gamma(\ )$ is the gamma function. Inverse Fourier transformation of $F(\omega)$ gives

$$\dot{\phi}(t) = \frac{1}{\Gamma(1-n)}\omega_{p,J}F_0 y^{-n} \times e^{-y}\,{}_1F_1(1-m; 2-n; y) \quad (45)$$

where $y = (\omega_{p,J}t)$. Integration of this equation, making use of the condition, Equation 2, that $\psi(0)$ is zero then yields

$$\psi(t) = \frac{1}{\Gamma(2-n)}F_0 y^{1-n} \times {}_2F_2(1-n+m, 1-n; 2-n, 2-n; y) \quad (46a)$$

and

$$\psi(\infty) = 1 \quad (46b)$$

Fig. 3a presents the form of the creep retardation function $\psi(t)$ and the retardation current, $\dot{\phi}(t)$ $(= \dot{\psi}(t))$, for a range of value of correlation indices m and n as given by Equations 46a and 45 respectively. The particular values of m and n used here have been chosen simply to indicate the type of behaviour that can be seen. Under the condition for which Equation 40 applies, $\gamma \to 1$, it can be seen that

$$\dot{\phi}(t) \simeq \dot{\theta}(t) \quad (47a)$$

and

$$\psi(t) \simeq \theta(t) - \theta(0) \quad ; \quad \gamma \to 1 \quad (47b)$$

Making use of these expressions the equivalent relaxation functions are presented in Fig. 3b. It is re-emphasized that the relations contained in Equations 47 are specific for the limit of γ approaching unity, that is a small dispersion process.

A more general approach to the form of the modulus functions can be indicated by equating the imaginary parts of Equation 32,

$$\frac{M(\infty)}{M_0}\frac{G''(\omega)}{[G'(\omega)]^2 + [G''(\omega)]^2} = \frac{J(\infty)}{J_0}\frac{F''(\omega)}{[F'(\omega)]^2 + [F''(\omega)]^2} \quad (48)$$

in which we have written

$$F(\omega) = F'(\omega) - iF''(\omega) \quad (49a)$$

and

$$G(\omega) = G'(\omega) - iG''(\omega) \quad (49b)$$

Equation 48 shows that as the frequency ap-

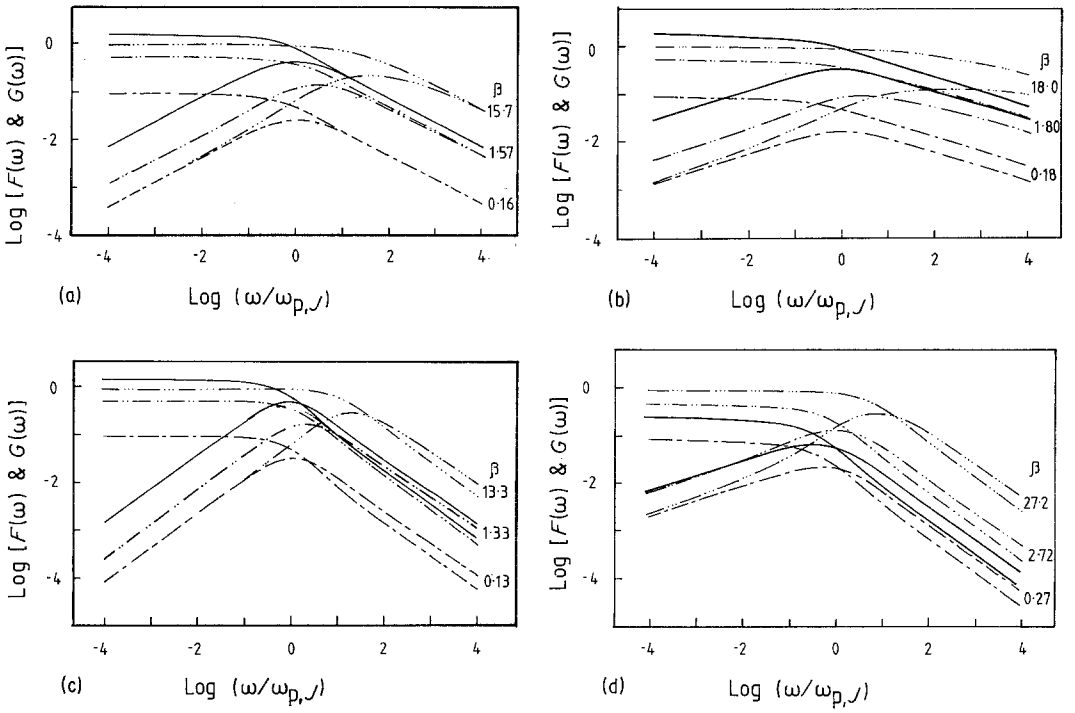

Figure 4 Computed transformation of $F(\omega)$ to give $G(\omega)$ from Equation 35. The function $F(\omega)$ is shown by the continuous plots. In this and the following two diagrams $G(\omega)$ as a function of β is indicated by the dashed plots with — — — — — $J(\infty) = 10$; —·—·— $J(\infty) = 1$; —···—···— $J(\infty) = 0.1$; and $J_0 = F_0$. The plots have been scaled to the characteristic relaxation rate $\omega_{p,J}$. The particular values of m and n have been arbitarily chosen to indicate the range of behaviour that can be observed: (a) $m = n = 0.5$; (b) $m = 0.3$, $n = 0.7$; (c) $m = 0.7$, $n = 0.3$; and (d) $m = n = 0.3$.

proaches zero

$$G''(\omega) \to F''(\omega) \cdot \gamma; \quad \omega \to 0 \qquad (50)$$

so that in *all* cases the low frequency loss modulus has the spectral form of the compliance loss in the same frequency region. For frequencies greater than the peak loss frequency of the compliance, $\omega_{p,J}$, we have already seen, in Section 2.4, that a similar one to one transformation cannot be achieved because of the shift in the modulus loss peak frequency into this region. However when $F(\omega)$ is of the form contained in Equation 42 [21]

$$F''(\omega) = F'(\omega) \cdot \cot(n\pi/2) \propto \omega^{-(1-n)}; \quad \omega \to \infty \qquad (51)$$

so that the right-hand side of Equation 48 has a spectral response of the form $\omega^{+(1-n)}$ which would be satisfied if the modulus function obeyed a similar relationship to that contained in Equation 51. This is obviously the case when γ approaches unity.

Fig. 4 shows the computed transformations of the compliance function in terms of the modulus spectral function $G(\omega)$ for a range of values of the ratio of compliances $J_0/J(\infty)$ which, for convenience, we set equal to β where

$$\beta = \gamma^{-1} - 1$$

using the same values of correlation indices as used in the previous figure. The features indicated in the previous discussion can be seen. In particular the equivalent gradients in the log–log plots of the loss components at frequencies below the loss maxima; the equivalent loss maxima frequencies when β is small ($\gamma \to 1$); and the distortion introduced into the modulus function as β increases. In Fig. 5 the complete modulus spectral response, $M(\omega)$, derived from the decrement plots of Fig. 4 are given and reinforce these observations.

The cooperative relaxation/retardation functions have been summarized in the Appendix for the cases considered above. The observation of power law behaviour in the asymptotic limits is a convenient technique for determining the

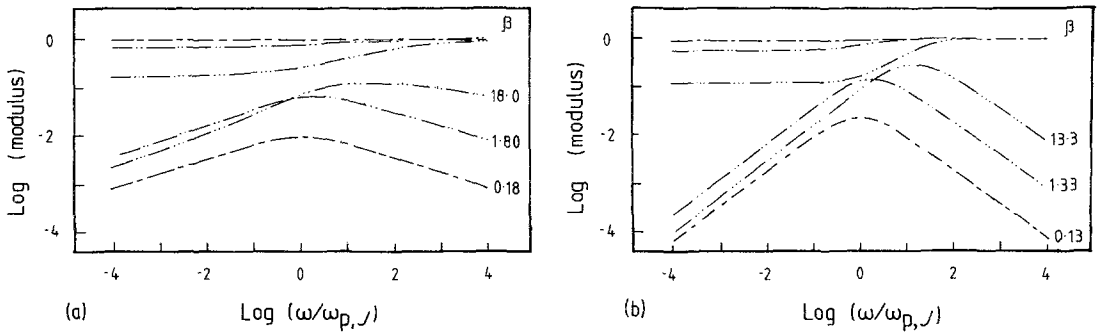

Figure 5 The modulus spectral response determined from the $G(\omega)$ response presented in Fig. 4b and c. The form of line marking is identical to that used in Fig. 4. (a) $m = 0.3, n = 0.7$; (b) $m = 0.7, n = 0.3$.

correlation indices of the cooperative behaviour and in the Appendix these limiting behaviours are indicated.

3.2. Viscous behaviour

The perfect viscous behaviour of a Newtonian liquid has been characterized in Equations 15, 19 and 23 as

$$\eta^{-1} = \alpha/\dot{\sigma}; \quad J(t)_\eta = t/\eta; \quad J(\omega)_\eta = -i(\omega\eta)^{-1}$$

from which the equivalence between the viscosity and electrical resistance is apparent as given in Table I. As we wish, in this section, to examine the effects of viscosity by itself we set J_0 in Equation 23 to zero, so that M_0 is also zero, and re-write Equation 30 in the form

$$\left[J(\infty) - \frac{i}{\omega\eta}\right] \cdot [M(\infty) - V_0 g(\omega)] = 1 \quad (52)$$

in order to obtain the effective spectral response of the viscosity in terms of the modulus as

$$V_0 g(\omega) = \frac{M(\infty)}{1 + i[\omega\eta/M(\infty)]} \quad (53)$$

Equation 53 describes a Debye-like behaviour of magnitude $M(\infty)$ and maximum loss frequency $\omega_{p,V} = M(\infty)/\eta$. This gives a sensitive test for the observation of Newtonian viscosity. Further we note that, as indicated earlier, in the presence of a viscosity there is *always* a frequency which is sufficiently small, say two orders of magnitude less than $\omega_{p,V}$, at which the magnitude of the modulus response approaches zero. The equivalent time can be considered as the time to reach the steady state which contains no stress.

3.3. Viscoelastic behaviour

Perfect relaxation behaviour is commonly observed under conditions of small stress and strain in metals whereas viscosity is commonly attributed to liquid-like materials. Viscoelastic behaviour which contains elements of both elasticity and viscosity is commonly observed in rubbers and plastics. In the modulus representation of viscoelastic response there is a peak in the loss component and both the real and loss components decrease to small values as the frequency tends to zero [22]. The essential difference on a compliance plot between viscoelastic behaviour and viscous behaviour is the dispersion in the *real* part of the compliance, c.f. Equation 52. It is just this pattern of behaviour in electrical relaxation studies that led Jonscher [12] to identify the anomalous low frequency dispersion as a separate type of relaxation response which, although it contains elements of charge transport, is not a d.c. conduction process. Fig. 6 contains plots of the modulus transformation of Equation 42 using negative values of m in the allowed range from zero to unity and the similarity to the broad pattern of the behaviour of viscoelastic materials is striking.

One feature of these plots is the position of the maximum in the loss component of the modulus. All the diagrams are scaled in frequency with reference to the characteristic frequency of the compliance function, $\omega_{p,J}$. For small values of β, and particularly as m approaches -1, it can be seen that $\omega_{p,M} < \omega_{p,J}$, in complete contrast to the condition derived for compliance loss peak behaviour and which is contained in Equation 39. In practice for strongly viscoelastic materials m does tend to approach its limiting value and hence it appears general that the viscoelastic modulus relaxation rate will be *less* than that of the equivalent compliance characteristic rate. We note,

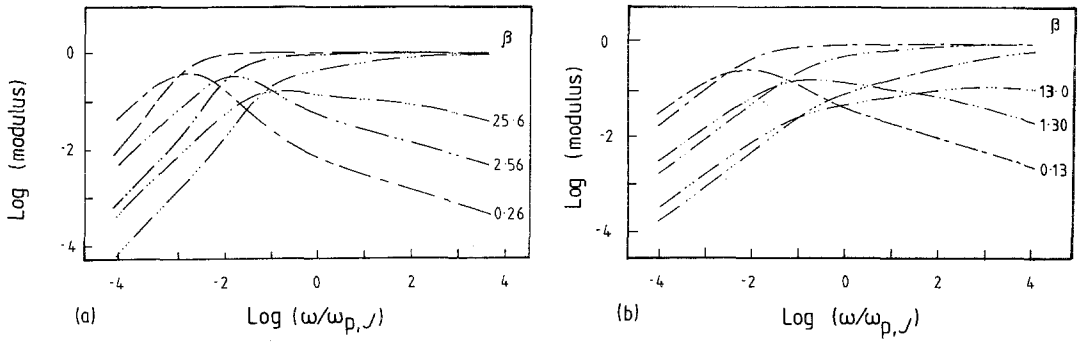

Figure 6 The modulus spectral response obtained by the transformation of the compliance function under conditions of anomalous low frequency dispersion. The line marking is as indicated in Fig. 4. (a) $m = -0.9$, $n = 0.7$; (b) $m = -0.7$, $n = 0.7$.

however, in all the cases considered here the actual relaxation rate for the modulus is *identical* to that for the compliance. It is the *assumption* that the peak loss frequency defines the relaxation rate that causes the apparent change in magnitude.

For completeness a further complication should be realized. Only in the case of symmetrical compliance loss peaks, that is when $m = 1 - n$ and an elastic response is being considered, is the peak in the compliance loss identical to the relaxation rate. In all other cases the skewness introduced into the loss characteristic shifts the peak loss value away from the characteristic frequency $\omega_{p,J}$ in the direction of lower gradient. This can be seen in Fig. 4 in which the relevant compliance function has been plotted as well as the modulus decrement spectral function. The shift, in this case, is relatively small even for quite asymmetric loss plots.

4. Experimental behaviour

The published literature on retardation and relaxation behaviour has been examined in order to obtain suitable experimental data by means of which a comparison with the theoretical functions derived in the previous section could be carried out. Unfortunately few materials appear to have been investigated by more than one experimental technique and hence none of the cases reported here allow a cross-check from one investigative technique to another to be made. The data has been chosen solely with the criterion that a good range of frequency/time should have been reported in order that a meaningful comparison with the theoretical functions might be made. The original units in which the information was presented have been retained. No particular emphasis has been placed on the frequency dependence of the compliance as this has already been the subject of a previous examination [17].

4.1. Strain retardation

Figs. 7 to 9 present data on the time dependence of the compliance. The data shown in Fig. 7 was obtained by Plazek and Magill [23] on 1:3:5 tri-α-naphthalene and has been normalized to the infinite time value of the compliance. The normalized plot presented here has been constructed from four sets of data in the temperature range 337.3 to 352.2 K, making no assumptions about

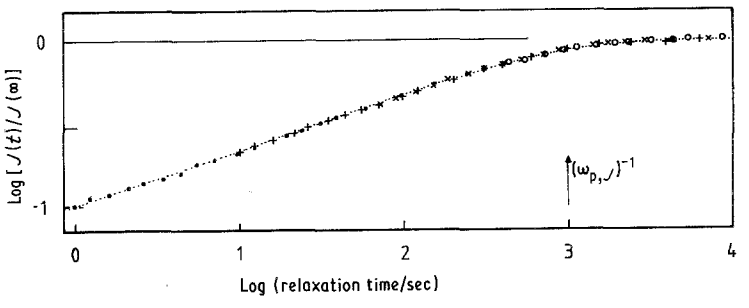

Figure 7 Creep relaxation in 1:3:5 tri-α-napthalene benzene normalized from the data of Plazek and Magill [23]. The plot through the data points is given by Equation 46 with $m = 0.9$ and $n = 0.66$. The diagram is scaled at 337.2 K. In this and the following two diagrams the relaxation rate $(\omega_{p,J})^{-1}$ is indicated. • 337.2 K; + 342.2 K; × 347.2 K; and ○ 352.2 K.

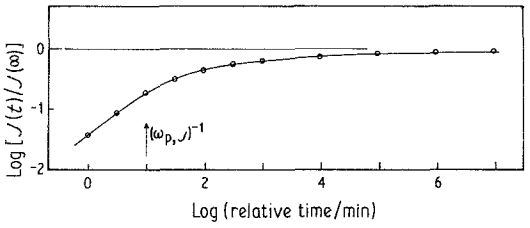

Figure 8 Creep relaxation in natural rubber from the data of Conant *et al.* [24]. The data points have been taken from a temperature normalized plot covering the range 213 to 304 K. This diagram is scaled for 213 K. The plot through the data is given by Equation 46 with $m = 0.1$ and $n = 0.29$.

the form of the temperature dependence of the relaxation rate. The plot through the experimental points is given by Equation 46 with $n = 0.66$ and m taken as 0.9. It was found that the function was relatively insensitive to the value of m although strongly sensitive, in the short time power-law region, to the value of n. The equivalent data shown in Fig. 8 was obtained from a shear experiment on natural rubber by Conant *et al.* [24] in the temperature range 213 to 304 K and the data here has been taken from the normalized plot that was presented. The theoretical curve in this case was computed with $n = 0.29$ and $m = 0.1$.

In Fig. 9 similar results obtained from a sample of polystyrene are shown. This data was measured by Plazek [25] who constructed this normalized plot from his data. Here the effect of a finite viscosity and a finite zero time compliance can be seen superimposed on the creep retardation curve. The computed creep characteristic, shown by the fine dashed plot, was obtained from Equation 46 with $m = n = 0.2$. As expected, Equation 19, the viscosity dominated region has a gradient of exactly unity in this log–log presentation.

The frequency dependence of the shear compliance of two rubbers is shown in Fig. 10 where the experimental data has been fitted to the spectral response function of Equation 43 with the values of the parameters m and n listed in the legend to the figure. It can be observed that in both cases the index n has a value close to 0.4 but that the crepe rubber has a slightly larger value of m than that exhibited by the butyl rubber. In neither case is there a significant effect from an "infinite frequency" value of the compliance, which has been taken as zero in the computation. The figure also indicates that the retardation rate in the crepe rubber is about fifteen times larger than that in the butyl. The information contained in this figure has been taken from the experimental work of Blizzard [26].

More complex frequency behaviour is indicated in Fig. 11 for two polymers, polyvinyl acetate [27] and poly-n-butyl methacrylate [28]. In both cases two dispersive processes occur in the frequency range covered by the normalized data. At the lower, relative, frequencies there are loss peaks just evident, indicative of an elastic response, whilst at higher frequencies anomalous compliance dispersions are dominant. It has been found possible, however, to construct theoretical fits to each of these processes individually, in both cases, as can be seen from the curves plotted through the experimental points. The region of transition from one

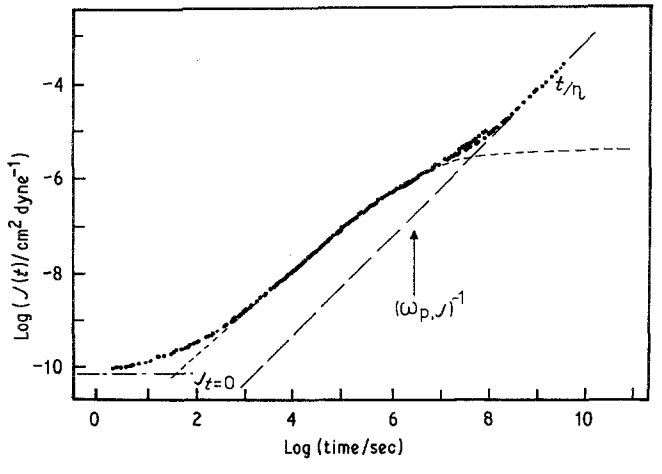

Figure 9 Creep relaxation in polystyrene from the normalized data of Plazek [25]. Both a viscosity and an initial compliance are indicated. The dashed curve through the creep relaxation response was obtained from Equation 46 with $m = n = 0.20$.

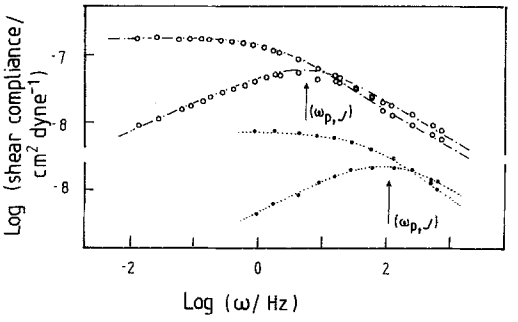

Figure 10 The frequency response of the shear compliance of two rubbers from the work of Blizzard [26]. The samples were measured at 278 and 293 K and the data have been taken from the temperature normalized plots. The curves through the data points are given by Equation 43 with the listed values for the parameters m and n. No evidence was found for an "infinite frequency" compliance. In this and the following five figures the characteristic rate constant, $\omega_{p,J}$, is indicated. ○ butyl rubber; —·—·— $m = 0.39$, $n = 0.41$; • crepe rubber; ····· $m = 0.45$, $n = 0.40$.

description to the other is indicated by the arrows in the diagrams and in this region there is an equivalence between the m and n values, $m = n - 1$, as indicated in the legend. Hence the complete fit of these complex responses has been made with only three free parameters.

4.2. Stress relaxation

The frequency response of the stress relaxation has been determined for the cooperative approach by making use of the transformation of Equation 37a and the response function contained in Equation 43. The computed spectral functions are given in Figs. 12 to 15. Fig. 12 presents the Young's modulus response of poly(4-chlorocyclohexyl acrylate) in the temperature range from 203 to 295 K from the data of Heijboer [29] in the form of a normalized plot. The small dispersion in the real part of the modulus indicates that the approximation $\gamma \to 1$ should apply and the figure shows

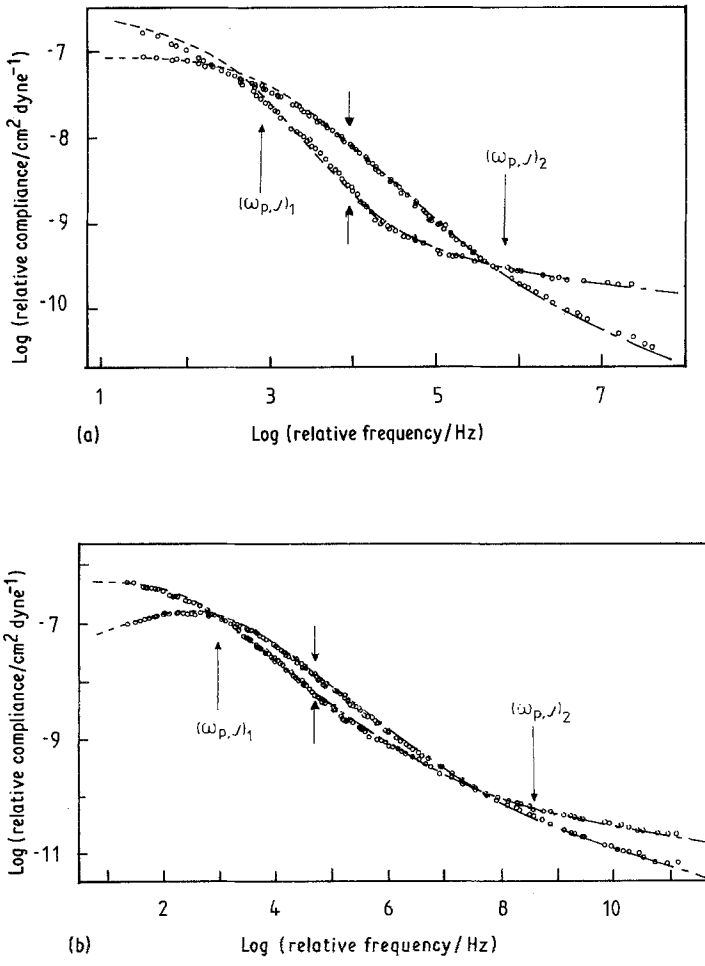

Figure 11 The normalized frequency response of the compliance of (a) polyvinyl acetate, and (b) poly-n-butyl methacrylate. In both cases the normalized plot covers a large relative frequency range and two relaxation processes can be seen, a loss peak at low frequencies and an anomalous dispersion at higher frequencies. In (a) the data has been taken from the work of Williams and Ferry [27]. The original measurements covered the temperature range from 223 to 363 K, the plot is scaled at 363 K and the theoretical curves are given by – – – – – $m = 0.01$, $n = 0.14$; ——— $m = -0.86$, $n = 0.53$, $\beta = 3.67$. For (b) the data was taken from Child and Ferry [28], the original temperature range was 317 to 343 K, the plot is scaled at 403 K, and – – – – – $m = 0.3$, $n = 0.3$; ——— $m = -0.7$, $n = 0.67$ with $\beta = 19.8$. The transitions between the processes are indicated by the double sets of arrows.

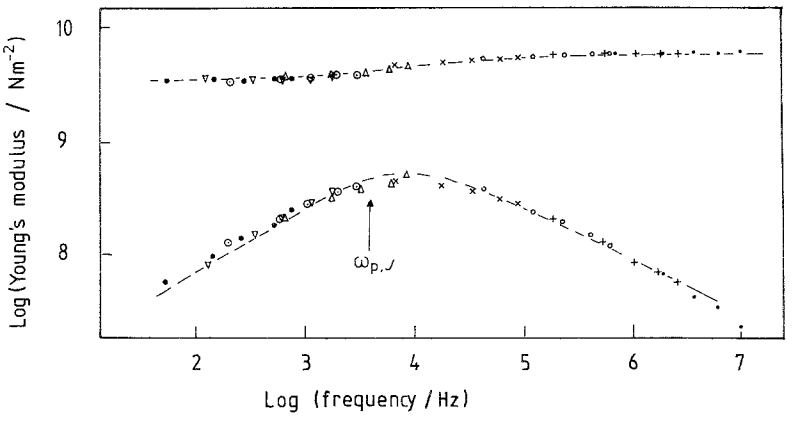

Figure 12 The normalized frequency response of Young's modulus in poly(4-chlorocyclohexyl acrylate). The data were measured in the temperature range between 203 and 295 K by Heijboer [29]. The diagram is scaled at 273 K and the plots through the data are given by the transformation of Equation 37a on the spectral function of Equation 43 with $m = 0.57$, $n = 0.50$ and $\beta = 1.03$.

the good fit to the experimental data that has been obtained taking $m = 0.57$, $n = 0.50$ and $\beta = 1.03$ ($\gamma = 0.49$). The data exhibited in Fig. 13 is taken from the experimental work of Read and Dean [14]. In Fig 13a both the tension and shear moduli of perspex at 294 K are plotted together with the spectral function given by $m = 0.135$, $n = 0.85$ and $\beta = 1.38$. The plot is scaled for shear and the modulus axis requires to be multiplied by a factor of 2.6 for the tension data. Fig. 13b shows a similar plot for the shear modulus response of unplasticized polyvinyl chloride at the same temperature, and in this case the values of the parameters used in computing the spectral function were $m = 0.22$, $n = 0.85$ and $\beta = 0.54$. In these three cases the spectral response of the loss component of the modulus is broad, typical of the behaviour of polymeric materials. Furthermore all three examples show behaviour which would transform into loss peak spectra in compliance, that is they are elastic responses with finite values of $M(0)$.

Viscoelastic behaviour is shown in Fig. 14 in linear polybutadiene, Fig. 14a, and hydrogenated linear polybutadiene, Fig. 14b. The former being taken from the work of Rochefort *et al.* [30] and the latter from the work of Raju *et al.* [31]. Both sets of data are characterized by large values of β ($\simeq 400$) and the effect of hydrogenation on the spectral response can only be seen as a small

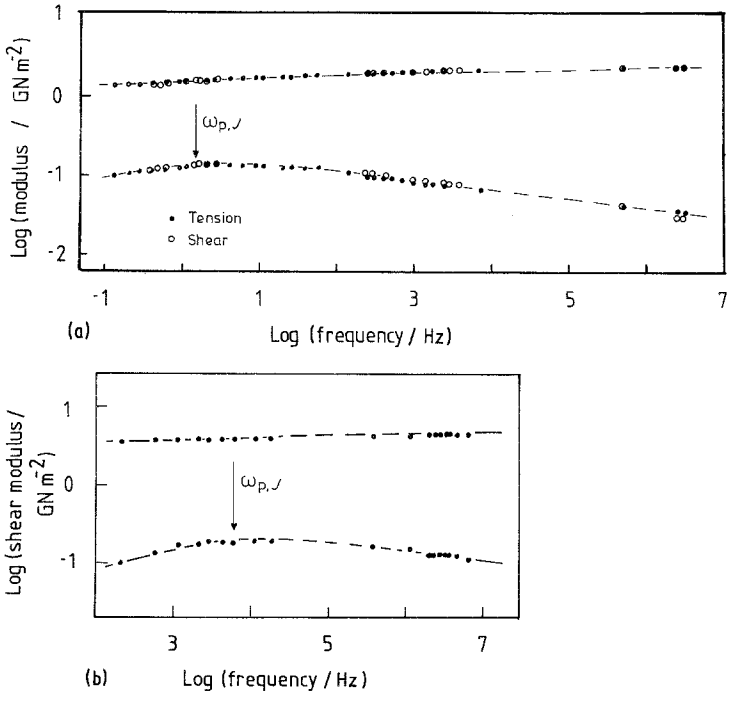

Figure 13 The frequency response of the modulus of perspex and polyvinyl chloride from the investigations of Read and Dean [14] at 294 K. (a) Perspex in shear and tension. The shear data requires to be multiplied by a factor of 2.6. $m = 0.135$, $n = 0.85$ and $\beta = 1.38$. (b) Unplasticised PVC. $m = 0.22$, $n = 0.85$ and $\beta = 0.54$.

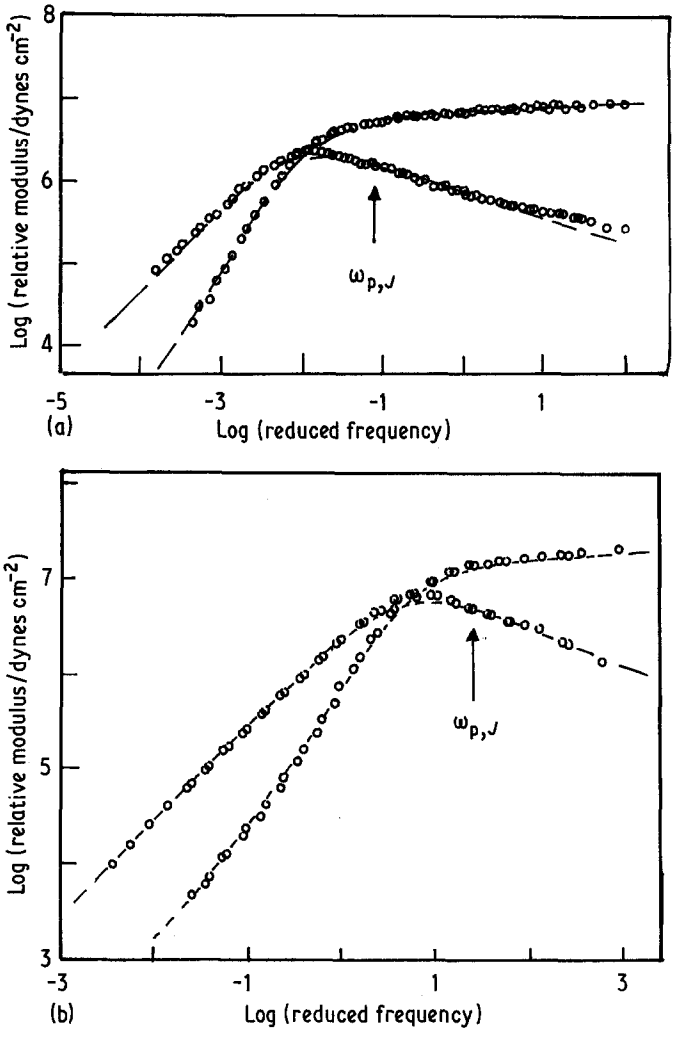

Figure 14 The frequency response of the modulus of two samples of linear polybutadiene. (a) A sample of molecular weight 791 000 [30], $m = -0.97$, $n = 0.68$ and $\beta = 415$. (b) A hydrogenated sample of molecular weight 360 000 [31], $m = -0.97$, $n = 0.5$ and $\beta = 420$.

change in n from 0.6 for the unhydrogenated material to 0.5 for the hydrogenated. The samples however had a 2:1 ratio of molecular weights and it is not possible to say, without further information, whether this or the hydrogenation is the cause of the slight difference in the values of n. One particular feature of interest here is the asymptotic behaviour of the modulus at low frequencies where both the imaginary and real components become parallel as shown in Fig. 14b. This can be contrasted with the equivalent low frequency behaviour exhibited by a sodium

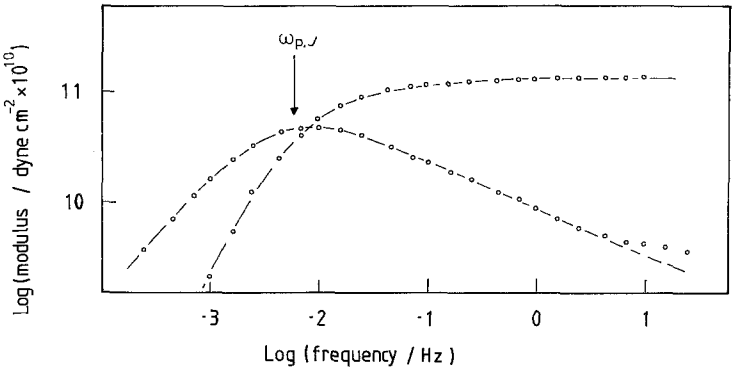

Figure 15 The frequency response of the modulus of a sample of $Na_2O:2SiO_2$ measured in the temperature range 687 to 785 K by Mills [32]. The data points presented here have been taken from the normalized modulus response curves. The function plotted through the data points is the combined response due to a perfect viscosity, of relative strength 0.45, and an elastic component with $m = 0.8$, $n = 0.6$ and $\beta = 1.12$.

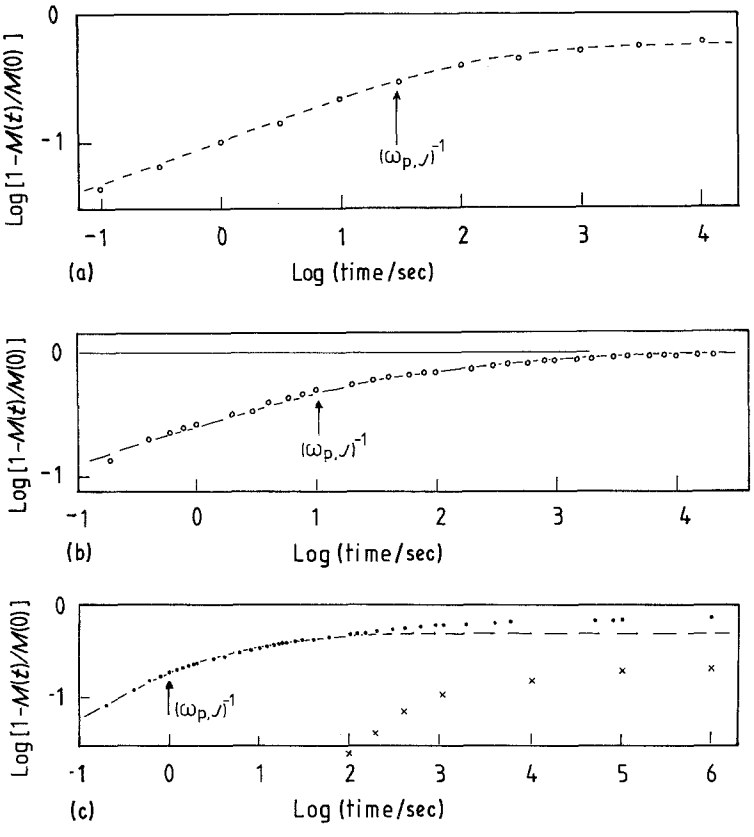

Figure 16 Stress relaxation in (a) aluminium, (b) cadmium, and (c) low density polyethylene, from the data of Kê [33] and Kubat [34]. The curves in these plots have been obtained by using Equation 54 and substituting $\phi(t)$ for $\theta(t)$. In the polyethylene case there is clear evidence for the existence of a second relaxation process at long times, the crosses having been obtained by taking the difference between the experimental data and the theoretical function. The parameters used in fitting the data were (a) $m = 0.1$, $n = 0.66$; (b) $m = 0.1$, $n = 0.7$; and (c) $m = 0.1$, $n = 0.46$. The apparent constancy of m is due to the insensitivity of the plots to this parameter. The plots show the time range of measurement and the equivalent relaxation time $(\omega_{p,J})^{-1}$ is indicated in each case.

silicate glass at high temperatures which is shown in Fig. 15. In this case there is a divergence between the real and imaginary components indicative of viscous behaviour. The theoretical curves through the data have been obtained with normalized parameters $m = 0.8$, $n = 0.6$, $\beta = 1.12$ and a viscosity, η, of 0.45, which indicates the parallel response of a perfect flow and a simple retardation effect which would give a compliance loss peak unlike the limited flow property exhibited by the polybutadiene in the previous figure. The data in Fig. 15 was obtained over the temperature range 687 to 785 K by Mills [32] and the points shown in the figure were taken from a normalized plot.

The time dependence of the stress relaxation is given by the inverse one-sided Fourier transformation of the modulus spectral relaxation function. Alternatively the assumption can be made that in the cases of interest γ approaches unity and Equations 40 and 47 apply. In this case the assumption can be tested by the degree of fit between experiment and the postulated theoretical response. It is this latter approach that we shall follow here. In obtaining Fig. 3d, the stress relaxation functions, it was found that the time evolution plot of stress relaxation was insensitive to the values of the cooperative parameters m and n, more so indeed than the similar insensitivity to m reported in this section for creep retardation. For this reason it has been found convenient to re-cast Equation 20 in the form

$$1 - \frac{M(t)}{M_i} = \frac{M_0}{M_i} \cdot \theta(t) \equiv \frac{M_0}{M_i} \cdot \phi(t) \qquad (54)$$

where the equivalence is the assumption to be tested.

Three plots of $[1 - M(t)/M_i]$ are presented in Fig. 16 for the experimental data of stress relaxation in aluminium [33], cadmium [34] and low density polyethylene [34]. In each case the curve through the data is $\phi(t)$ as given by Equation 45, and using the parameters listed in the legend to the figure. Very good agreement has been obtained for aluminium and cadmium. In the case of the polyethylene there is clear evidence for a second, weaker, stress relaxation process on a time scale that is about four orders of magnitude greater than the principal relaxation. In Fig. 16c

the crosses have been obtained by plotting the difference between the experimental curve and the theoretical function. In all three cases it has been found, as for creep retardation, that the plots are relatively insensitive to the value of m nevertheless it can be seen that in all cases the initial stress decay is of a fractional power law in time form.

5. Discussion

The approach followed in Section 2 reflects the conventional development of the constitutive equations and the convolution integral of mechanical response [1, 2]. However in order to carry out the comparison with experimental data which is presented in Section 4 it was found necessary to evaluate the exact significance of the initial and final retardation/relaxation states. It is believed that the constitutive equations presented here, Equations 5 to 10, are a correct representation of the creep and stress relaxation functions, and that Equations 27 and 29 correctly interpret the interrelationships between the compliance and modulus in elastic and viscoelastic materials. The approach developed here differs from the conventional formalism by setting the response of a particular process within the framework of a general retardation/relaxation which contains more than one process. This is experimentally substantiated by, for example, the observation that of the ten systems investigated in the frequency domain only two, the butyl and crepe rubbers, indicate a negligible value for the infinite frequency compliance. In all other cases it has not been possible to consider the observed relaxation process in isolation. A further support for the general approach is given by the stress relaxation data where the finite initial value of the stress, M_i, necessitates a zero time response of the system.

The feature of the analytical development contained in Section 3 is the assumption of the applicability of the cooperative approach to dielectric relaxation [8–10, 15, 16] to the field of mechanical retardation/relaxation. The previous investigation [17] had indicated the applicability in terms of the frequency response of the loss component of the anelastic compliance. Here the investigation has been extended to creep retardation, stress relaxation and the full spectral response of both compliance and modulus. For the stress relaxation case it has been assumed that the dispersion parameter γ approached unity. For the stress relaxation data there is no evidence of viscoelastic behaviour and with the metals it is known that there is a finite value of residual stress after the relaxation has been completed and a zero time relaxation is expected. Hence the assumption is justified as has been shown by the degree of fit obtained for these cases. For polyethylene it has been shown elsewhere [35] that the magnitude of the dispersion in the compliance arising from the equivalent process is small and hence here too the assumption is justified.

All the experimental data examined have exhibited non-Debye behaviour. The conventional approach to this observation is to consider a distribution of Debye-like retardation/relaxation elements to be present in the material. Gross [1] has given a detailed account of the results of this assumption, and in particular has pointed out that the retardation spectrum of the distribution differs from the relaxation distribution for the same initial set of experimental data, whether these be in compliance or modulus form. Seldom has the initial assumption of a distribution of responding elements been questioned. It should be understood that the description of the response of the system in terms of either a retardation or relaxation spectrum is purely a mathematical transformation of the experimental data *unless* the spectra can be associated with some other distributed property of the system. This association has not been made in either mechanical or dielectric investigations and hence there is little real support for the assumption itself. Furthermore, if we consider the distribution spectra as a model for the cooperative nature of the response of solids then it is a severely limited model for it assumes that each individual element, characterized only by its relaxation time, acts *independently* of all the other elements with the same or different relaxation time. The independence which is built into the Debye model only allows interaction through a viscous damping which, itself, characterizes the relaxation time of the element. To our knowledge the only systems which exhibit true Debye behaviour are weak polar gases.

The cooperative approach followed here makes use of a system averaged characteristic relaxation rate and correlation parameters which are associated with two specific forms of cooperative dynamics, namely, inter-cluster cooperative motions and intra-cluster cooperative exchanges [16]. In Section 4

it has been shown that these three parameters, together with a magnitude of response, are sufficient to completely define the observed response of a single process of relaxation/retardation. In this approach the broadening of the single particle Debye response is a result of the internal cooperative motions, so that the measured response is a system average and not an average of individual systems. In this context it can be pointed out that the inverse relationships of Equations 35 and 36 arise from consideration of the equation of motion of a coupled system and represent over-damping of a system resonance.

The validity of the assumption of the cooperative model has been substantiated by the degree of agreement between the model and the wide range of experimental data reported in the previous section. The significance of this observation will be examined elsewhere but for the present we consider that the cooperative relaxation model is as applicable to mechanical relaxation as it is to dielectric relaxation. The observation of two distinct classes of behaviour, loss peak behaviour in compliance, which gives rise to limited dispersion in the modulus and can be associated with limited structural reorganisation, and anomalous low frequency dispersion in compliance, which gives complete annihilation of the modulus at zero frequency and which can be associated with limited flow in the system, gives support to the use of elasticity and viscoelasticity as descriptions of retardation/relaxation behaviour. In the former case the compliance description is pertinent and in the latter the modulus representation is relevant. Other forms of data presentation are equally possible, for example in a viscosity dominated response a complex and frequency dependent viscosity can be derived [2] and used as a convenient method of representation. The essential feature, however, is the commonality of the response of a system to different mechanical stresses and strains. Such presentations should be considered only as an aid to delineating specific features of the response of the system and not as a description of the response.

One particular point in the use of data presentation has been examined in some detail. This is the evaluation of the relaxation rate by means of evaluation of the maximum in the loss plots. It has been shown that such a definition only applies rigorously under elastic conditions and when $m = 1 - n$ in compliance form. When the dispersion is small, that is when the magnitude of the peak loss is much less than the weakly dispersive real part, then the modulus form can be used under the same symmetry condition. In all other cases the skewness of the loss spectral form shifts the frequency of peak loss away from the true characteristic frequency and towards the frequency region of lower slope in a log–log presentation. On transformation into a modulus spectrum where the maximum loss is not small the frequency shift can be large and is dependent on the relative magnitude of the process under investigation and of the type of process. Under elastic conditions we expect the frequency of maximum modulus loss to be greater than the true retardation rate, whereas under viscoelastic conditions the converse will apply. However if the spectral shape in either compliance or modulus is unchanged under the action of an external variable such as temperature the *relative* shift of the peak loss can be used in the evaluation of the change in the characteristic rate under the action of the variable. The error in the characteristic rate appearing in the absolute value.

6. Conclusions

The mechanical relaxation response functions have been generalized in order to evaluate the significance of the initial and final relaxation states in real materials. This has allowed the anelastic responses to be examined and analytic transformation functions between compliance and modulus to be established. The applicability of the cooperative model of relaxation has been substantiated by making a detailed comparison with experimental data over a wide range of material types and techniques of investigation. It follows that the elastic behaviour is governed by limited configurational relaxations in the material, which are equivalent to the local structural reorganisations that take place in dielectric relaxation in the region of active dipoles. Furthermore the presence of viscoelastic behaviour has been shown to be an imperfect flow property and analogous to the anomalous low frequency dispersion process which has been observed dielectrically in materials containing free ions. In the limit of free flow the mechanical response is dominated by a totally real viscosity, just as direct current conduction dominates the electrical response under the equivalent "free carrier" conditions.

Acknowledgements

The author gratefully acknowledge helpful discussions with Dr W. G. G. Britton on the Physics Department, Chelsea College.

Appendix: mechanical response functions

1. Creep retardation function

$$J(t) = J_0 F_0 \frac{y^{1-n}}{\Gamma(2-n)} {}_2F_2 \times (1-n+m, 1-n; 2-n, 2-n; -y) \quad \text{(A1)}$$

limit approximations

$$y > 1 \quad 1 - \frac{J(t)}{J_0} = a \cdot y^{-m} \quad \text{(A1a)}$$

$$y < 1 \quad \frac{J(t)}{J_0} = F_0 \frac{1}{\Gamma(2-n)} y^{1-n} \quad \text{(A1b)}$$

2. Spectral response of compliance

$$J(\omega) = J'(\omega) - iJ''(\omega) = J_0 F(\omega) + J(\infty)$$

with

$$F(\omega) = F_0 (1+ix)^{m-1} \times {}_2F_1 \left(1-n, 1-m; 2-n; \frac{1}{1+ix}\right) \quad \text{(A2)}$$

limit approximations

$$x > 1 \quad F'(\omega) \propto F''(\omega) \propto \omega^{n-1} \quad \text{(A2a)}$$

$$x < 1 \quad F(0) - F'(\omega) \propto F''(\omega) \propto \omega^{m} \quad \text{(A2b)}$$

3. Spectral response of modulus

$$M(\omega) = M'(\omega) - iM''(\omega) = M(\infty) - M_0 G(\omega)$$

with

$$G(\omega) = \frac{J(0)}{J(\infty)} \left\{ [F(\omega)]^{-1} + \frac{J_0}{J(\infty)} \right\}^{-1} \quad \text{(A3)}$$

limit approximations

$$x \gg 1 \quad G'(\omega) \propto G''(\omega) \propto \omega^{n-1} \quad \text{(A3a)}$$

$$x < 1 \quad G''(\omega) \propto \omega^{m} \quad \text{(A3b)}$$

4. Stress relaxation function

For $M_0 \ll M_i$

$$\frac{M(t)}{M_i} \simeq 1 - \frac{J(t) M_0}{J_0 M_i} \quad \text{(A4)}$$

limit approximations

$$y > 1 \quad \frac{M(t)}{M_i} \simeq \left(1 - \frac{M_0}{M_i}\right) + \frac{M_0}{M_i} a y^{-m} \quad \text{(A4a)}$$

$$y < 1 \quad 1 - \frac{M(t)}{M_i} \simeq \frac{M_0}{M_i} \frac{F_0}{\Gamma(2-n)} y^{1-n} \quad \text{(A4b)}$$

Where $y = \omega_{p,J} t$; $x = \omega / \omega_{p,J}$; ${}_2F_2(\ )$ and ${}_2F_1(\ )$ are hypergeometric functions; $\Gamma(\ )$ is the gamma function; $F_0 = \Gamma(1-n+m)/[\Gamma(m) \cdot \Gamma(2-n)]$; and n and m are the correlation indices for two specific mechanisms of relaxation/retardation. J_0 is the magnitude of the compliance dispersion with infinite frequency value $J(\infty)$ and zero frequency value $J(0)$ so that $J(0) = J_0 + J(\infty)$. The time dependence of the compliance has been expressed as $J(t)$ with a defined zero time value of zero. M_0 is the magnitude of the modulus dispersion with infinite frequency value $M(\infty)$ and zero frequency value $M(0)$ so that $M(0) = M(\infty) - M_0$. The time dependence of the modulus has been expressed as $M(t)$ with an initial time value of M_i. The parameter a is a positive constant.

References

1. B. GROSS, "Mathematical Structure of the Theories of Viscoelasticity (Hermann, Paris, 1968).
2. J. D. Ferry, "Viscoelastic Properties of Polymers", 2nd edn (Wiley and Sons, New York, 1970).
3. S. HAVRILIAK and S. NEGAMI, *J. Polym. Sci.* **C14** (1966) 99.
4. K. S. COLE and R. H. COLE, *J. Chem. Phys.* 9 (1941) 341.
5. D. W. DAVIDSON and R. H. COLE, *ibid.* 19 (1951) 1484.
6. R. M. FUOSS and J. G. KIRKWOOD, *J. Amer. Chem. Soc.* **63** (1941) 385.
7. R. M. HILL, *Phys. Status Solidi (b)* **103** (1981) 319.
8. L. A. DISSADO and R. M. HILL, *Nature* **279** (1979) 685.
9. *Idem, Phil. Mag.* **B41** (1981) 625.
10. *Idem, J. Mater. Sci.* **16** (1981) 638.
11. V. V. DANIEL, "Dielectric Relaxation" (Academic Press, London, 1967).
12. A. K. JONSCHER, *Phil. Mag.* **B38** (1978) 587.
13. J. M. C. DUHAMEL, *J. Ec. Polytech.* **22** (1833) 1.
14. B. E. READ and G. DEAN, "The Determination of the Dynamic Properties of Polymers and Composites" (Hilger, Bristol, 1978).
15. L. A. DISSADO, *Physica Scripta* **T1** (1982) 110.
16. L. A. DISSADO and R. M. HILL, *Proc. Roy. Soc.* **A390** (1983) 131.
17. R. M. HILL, *J. Mater. Sci.* 17 (1982) 3630.
18. L. C. SLATER, "Confluent Hypergeometric Functions" (Oxford University Press, Oxford, 1960).

19. *Idem*, "Generalised Hypergeometric Functions" (Oxford University Press, Oxford, 1966).
20. L. A. DISSADO and R. M. HILL, *J. Chem. Soc. Faraday Trans.* to be published.
21. A. K. JONSCHER, *Colloid Polym. Sci.* **253** (1975) 231.
22. J. WONG and C. A. ANGELL, "Glass Structure by Spectroscopy" (Dekker, New York, 1976) Chap. 11.
23. D. J. PLAZEK and J. H. MAGILL, *J. Chem. Phys.* **45** (1966) 3038.
24. F. S. CONANT, G. L. HALL and W. J. LYONS, *J. Appl. Phys.* **21** (1950) 499.
25. D. J. PLAZEK, *J. Chem. Phys.* 69 (1965) 3480.
26. R. B. BLIZZARD, *J. Appl. Phys.* **22** (1951) 730.
27. M. L. WILLIAMS and J. D. FERRY, *J. Colloid. Sci.* 9 (1954) 479.
28. W. C. CHILD and J. D. FERRY, *ibid.* **12** (1957) 317.
29. J. HEIJBOER, TNO Communications No. 435, Delft (1972).
30. W. E. ROCHEFORT, G. C. SMITH, H. RACHAPADY, V. R. RAJU and W. W. GRAESSLEY, *J. Polym. Sci: Polym. Phys. Ed.* 17 (1979) 1197.
31. V. R. RAJU, H. RACHAPADY and W. W. GRAESSLEY, *J. Polym. Sci: Polym. Phys. Ed.* 17 (1979) 1223.
32. J. J. MILLS, *J. Non-Cryst. Solids* **14** (1974) 255.
33. T. S. KÊ, *Phys. Rev.* 71 (1947) 533.
34. J. KUBAT, "International Conference on Rheology, 1963" (Interscience, New York, 1965) p. 281.
35. T. KYU, N. YASUDA, S. SUEHIRO, T. HASHIMOTO and H. KAWAI, *Polymer* **21** (1980) 1205.

Received 9 August
and accepted 13 September 1983